AD-A269 827

Topographic Jetogenesis and Transitions in Straits and along Continents

MELVIN E. STERN

DTIC
ELECTE
SEP 28 1993
S B D

93-22405

COPY

Topographic Jetogenesis and Transitions in Straits and along Continents

MELVIN E. STERN

Department of Oceanography, The Florida State University, Tallahassee, Florida

ABSTRACT

When a low Rossby number barotropic flow accelerates in the laterally converging half of a strait, the local propagation speed of long topographic waves can be reduced to zero, thereby blocking or preventing the formation of a steady flow downstream from the strait. An inviscid longwave theory is presented for the new steady upstream and downstream states that evolve from the blocking wave. The enhanced inshore cyclonic vorticity extending far downstream suggests that topographic jetogenesis, rather than lateral eddy diffusion, in major ocean straits (e.g., Yucatan and Florida) may be important in generating or reforming boundary currents.

1. Introduction and simple considerations

Steady barotropic currents tend to follow continental isobaths when the curvature and the Rossby number R are sufficiently small. In a region of converging isobaths mass conservation requires the downstream velocity to increase, and potential vorticity conservation requires cross-isobath motions to account for the relative vorticity changes. Thus the velocity field in a converging channel can increase to a critical state such that the local propagation speed of long topographic waves vanishes, in which case no steady downstream state exists for the given upstream flow. A theory will be developed for the new upstream and downstream state as a function of the topographic convergence.

The "blocking" effect that occurs when the flow becomes topographically critical is analogous to that in classical, nonrotating open channel hydraulics (Long 1972) when an obstacle is towed along the bottom of an otherwise resting layer of water with a speed greater than that of long surface gravity waves. A wave of elevation then forms with its trailing edge fixed near the obstacle, and with its leading edge propagating ahead of the obstacle. In this way a new upstream state with an increased water level is produced, as well as a new (supercritical) downstream state. Similar effects occur in a rotating stratified fluid when it is blocked, and here it is the Kelvin wave propagation that is relevant. [See the reduced gravity model of Gill (1977).]

The control effect of continental topography on a parallel current has been studied by several authors. Hughes (1985, 1986, 1987) has computed particular "conjugate" flow states, for stratified as well as baro-

Corresponding author address: Melvin E. Stern, Department of Oceanography, B-169, The Florida State University, Tallahassee, FL 32306-3048.

tropic flow, having the same specified potential vorticity on the same streamline. Hydraulic transitions between such end states are possible, but the theory does not address the question of the new upstream and downstream states that evolve when an arbitrary upstream flow is blocked. In that case the spatial distribution of an entire *field* of potential vorticity is modified, so that the problem becomes more difficult than the classical one (Long 1972) in which only one or two parameters (e.g., the fluid height) are necessary to describe the upstream state. For this reason it is desirable to restrict our problem to very simple fields of upstream potential vorticity, such that only a finite number of degrees of freedom are involved in its modification. Herein lies the importance of piecewise uniform potential vorticity flow in the following inviscid, barotropic, and f-plane model.

Let us start by considering the steady flow shown in Fig. 1, in which the distinctive feature of the topography is the relatively large convergence of the isobaths near the central axis of the channel, as compared with the convergence near the sidewalls. The downstream (x^*) gradient of isobathic depth $h^*(x^*, y^*)$ is assumed small compared to the cross-isobath (y^*) gradient, so that $-\partial u^*/\partial y^*$ may be used as the long-wave approximation for the relative vorticity, where u^* is the dimensional downstream velocity, and $v^* \ll u^*$ is the y^* velocity component. Far upstream in Fig. 1 a uniform $u^* = U_0^*$ is assumed, with Rossby number $U_0^*/fW^* \ll 1$, where $f > 0$ is the Coriolis parameter. Under this condition a first approximation to the law of conservation of potential vorticity requires the steady streamlines to coincide with the isobaths, as previously mentioned. To conserve mass between laterally converging isobaths the velocity U^* on the central axis must increase relative to U_0^*, whereas the wall velocities U_1^*, U_2^* change less. This implies that a jet forms in

the converging half of the strait, with the necessary relative vorticities being produced by cross-isobath stretching or squashing of columns. Thus the cyclonic vorticity at P_1 (Fig. 1) and the anticyclonic vorticity at P_2, require cross-slope displacements as indicated by the arrows.

All but one of the following calculations will be done for models (Fig. 2) in which the smooth continental slopes are replaced by escarpments (the dashed curves), across which the nondimensional depth changes discontinuously from $h = 1$ to $h = \beta > 1$. The lateral length scale is some W^*, chosen (as convenient) to make either W_0 or W_1 or W_2 equal to unity in Fig. 2, and the nondimensional $D(x)$ gives the downstream (x) variation in width of the deepest part of the channel (the distance between escarpments). The uniform upstream speed U_0^* is the velocity scale, U_0^*/W^* is the vorticity scale, and the Rossby number is $R = U_0^*/fW^*$.

The main problem is to predict the steady flow having three piecewise uniform potential vorticity layers, and a given total volume flux at each x. These three layers are separated by two interfaces whose displacements L_1, L_2 from their respective escarpments are tentatively assumed positive in the $-y$ direction (to anticipate the jetlike profile in Fig. 2).

Since the upstream relative vorticity vanishes, and since potential vorticity is conserved, the cross-escarpment stretching $(\beta - 1)$ of columns in the L_1 layer produce the nondimensional vorticity

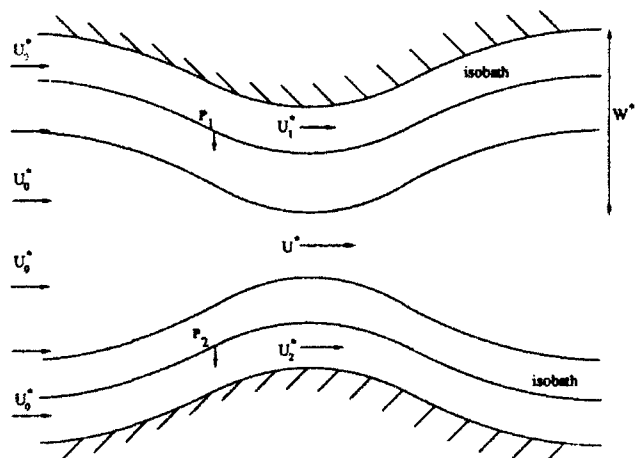$$\zeta = \frac{\beta - 1}{R}. \tag{1.1}$$

FIG. 1. Schematic diagram for steady, subcritical (low upstream Rossby number) barotropic flow through a strait. The sketched isobaths converge more rapidly in midchannel than the isobaths near the shores. The "zero-order" tendency for the flow to follow the isobaths suggests a large U^* must form in the highly convergent central portion of the straits. The implied relative vorticities require cross-isobath displacements at points P_1 and P_2 as shown by the arrows; W^* is a characteristic channel width (dimensional).
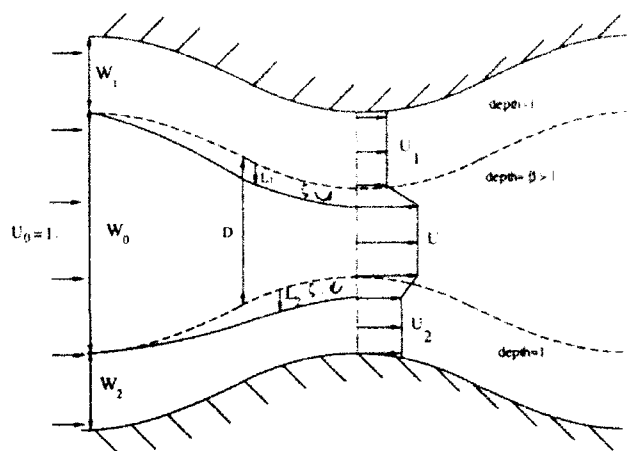

FIG. 2. An escarpment model as a limit of Fig. 1. The depth is uniform on the two "shelves" of uniform nondimensional widths W_1, W_2. The nondimensional depth increases (discontinuously) from unity to β across the escarpments (dashed). Cyclonic vorticity ζ is generated in the strip of width L_1 located between the upper escarpment and the interface (solid curve) separating the layers of uniform potential vorticity. Anticyclonic vorticity is generated in the L_2 layer.

Likewise, the *magnitude* of the anticyclonic vorticity in the L_2 layer is $\zeta_- = (1 - \beta^{-1})/R$, or

$$\beta\zeta_- = \zeta. \tag{1.2}$$

According to the long-wave approximation the downstream velocity varies linearly in these two vortical layers, and outside the velocities U_1, U, and U_2 are independent of y, where U is the uniform velocity in the central region, U_1 is the *upper-shelf* velocity, and U_2 is the *lower-shelf* velocity.

It is instructive to consider first the simplest example, in which both W_1, W_2 are much larger than $W_0 = 1$, in which case mass conservation in the relatively wide regions (W_1, W_2) requires $U_1 = U_2 \approx 1$. Adding this to the appropriate shear [Eq. (1.1) or (1.2)] gives the velocity U between the two interfaces

$$1 + \zeta L_1 = U = 1 + L_2\zeta_-, \tag{1.3}$$

and then Eq. (1.2) yields

$$L_2 = \beta L_1. \tag{1.4}$$

At any section x the total volume transport between the two interfaces is the sum of two parts, one of which $[\beta U(D - L_1)]$ occurs in deep water, and the other $[\frac{1}{2}(U + 1)L_2]$ occurs in the shallow anticyclonic layer. This sum is independent of x and equal to the transport $\beta W_0 = \beta$ at $x = -\infty$, so that

$$1 = (1 + \zeta L_1)(D - L_1) + (1 + \zeta L_1/2)L_2/\beta.$$

The use of (1.4) then gives the quadratic equation

$$L_1^2 - 2DL_1 + 2(1 - D)/\zeta = 0 \tag{1.5}$$

and the solution satisfying $L_1 = 0$ when $D = 1$ is

$$L_1 = D - (D^2 - 2(1 - D)/\zeta)^{1/2}. \quad (1.6)$$

This is positive because $D(x) < 1$, and thus our initial assumption $L_1 > 0$, $L_2 > 0$ is verified. The discriminant of the quadratic vanishes at a section where

$$D(x) = -\frac{1}{\zeta} + \left(\frac{1}{\zeta^2} + \frac{2}{\zeta}\right)^{1/2} < 1,$$

in which case $L_1 = D$, $L_2 = \beta D$, and consequently a triangular jet forms having a maximum velocity

$$U = 1 + \zeta L_1 = (1 + 2\zeta)^{1/2} = \left(1 + \frac{2(\beta - 1)}{R}\right)^{1/2}$$

located on the lower escarpment. If $R = U_0^*/fW_0^* \ll 1$, where the central channel width W_0^* now provides the W^* scale, this U is very large compared to the upstream current, and thus we see that pronounced inviscid jetogenesis can occur in the laterally converging half of a channel. The large values of the cyclonic and anticyclonic vorticities may then cause *separation* as the jet enters the diverging half of the channel (Stern and Whitehead 1990). This is one kind of transition that would prevent a reversal of the vorticity generation in the diverging half of the strait, and that would allow a jet to appear far downstream.

For the smaller W_1, W_2 (narrower shelves in sections 2 and 3), a hydraulic transition or blocking can occur first, and the single shelf ($W_2 = 0$) model in section 2 will address the main question, namely, what happens if $\min D(x)$ is small enough to block the uniform upstream current.

Both kinds of transition seem to be relevant to the influence of major ocean straits on the circulation in the basins they connect. One example is the Atlantic western boundary current, which appears to become very diffuse (and remote from boundaries) after entering the Caribbean Sea, and until it reforms as a jet in the vicinity of the Straits of Yucatan (Gordon 1967; Molinari et al. 1981). This Gulf Stream jet then passes through the Gulf of Mexico, and enters the Straits of Florida where the maximum mean *inshore* vorticity increases to a value approximately equal to the Coriolis parameter (Brooks and Niiler 1977). It is unlikely that this large inshore vorticity can be correctly explained by a lateral *diffusion* mechanism and a proper explanation should be based on an inertial (potential vorticity conserving) mechanism, taking into account the isobaths (and the isopycnals) in the strait (Stern 1991).

2. A converging channel with a single escarpment

In Fig. 3a W_2 has been set equal to zero, $W_0 = 1$ is the length unit, and $D(x) \leqslant 1$ is the distance between the curved lower wall and the escarpment. Note that in a long-wave theory the curvature of isobaths is unimportant, compared to their y separation, so that Fig.

3a is dynamically equivalent to Fig. 2 when $W_2 = 0$. (Such a model might be realized in a long rotating channel by towing an obstacle placed on a wall through an otherwise resting liquid.) In this case a single interface separates two regions of uniform potential vorticity, and $R = U_0^*/fW^*$ and β are first assumed to be such that a steady long-wave solution exists with $L = L(D(x)) \geqslant 0$. As previously indicated (1.1), the relative vorticity immediately above this interface is

$$\zeta = \frac{\beta - 1}{R} > 0 \quad (2.1)$$

and below the interface the velocity U is independent of y. The local volume transport $U(D - L)\beta$ in the latter region must equal the value (β) at $x = -\infty$, and therefore

$$U = \frac{1}{D - L}. \quad (2.2)$$

The shear above the interface (Fig. 3a) gives the velocity

$$U_1 = U - \zeta L \quad (2.3)$$

at and above the escarpment. Therefore the total volume transport above this interface is $U_1 W_1 + \frac{1}{2}(U_1 + U)L\beta$, and the latter must equal the transport W_1' at $x = -\infty$. Simplification of this equality using (2.2)–(2.3) yields

$$1 = \frac{1 + L\beta/W_1}{D - L} - \zeta L - \frac{\beta L^2 \zeta}{2W_1}, \quad (2.4a)$$

$$D = L + \frac{1 + L\beta/W_1}{1 + \zeta L + \beta L^2 \zeta/2W_1}. \quad (2.4b)$$

The implicit solution (2.4b) for $L = L(D)$ reduces to $D = 1 + L(\beta/W_1 - \zeta + 1) + \cdots$ when $L \to 0$, and since $D < 1$ a necessary condition for the $L > 0$ assumption is

$$\zeta > 1 + \beta/W_1 \quad (2.5a)$$

or

$$R < \frac{\beta - 1}{1 + \beta/W_1}. \quad (2.5b)$$

The right-hand side of (2.4b) is positive and asymptotes to $D = L$ when L is large, so that a minimum $D = D_c$ exists. This point separates two branches (Fig. 3b) having different L values for the same D, and if $\min D < D_c$ no steady solution exists for the upstream flow with uniform velocity.

For relatively large W^{-1} Eq. (2.4a) reduces to a quadratic equation

$$L^2 - L\left(D - \frac{1}{\zeta}\right) + (1 - D)/\zeta = 0 \quad (2.6)$$
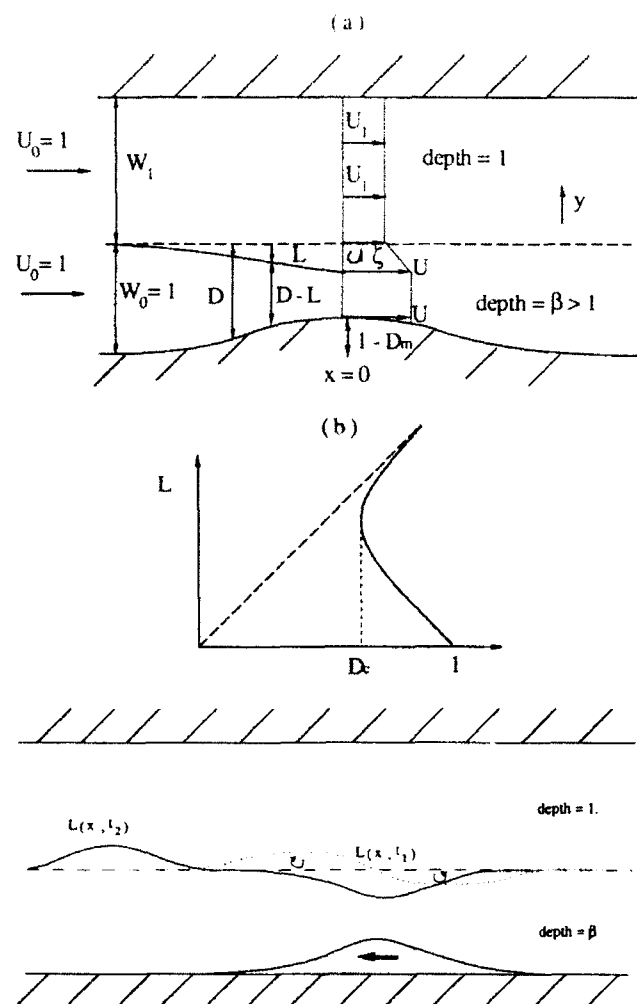
FIG. 3. (a) Flow of a uniform upstream current $U_0 = 1$ in a channel with a single escarpment (dashed horizontal line). The distance $D(x)$ of this from the lower vertical wall varies slowly on the $W_0 = 1$ length scale. The interface between the piecewise-uniform potential vorticity layers is displaced downward (negative y) by an amount $L(x) > 0$ in the steady state. Above the interface nondimensional vorticity ζ is thereby generated, and the velocity varies linearly between the values U_1 and U. (b) Sketch of a long wave solution for L as a function of D. The branch point at $D = D_c$ is the smallest value possible for a given Rossby number at $x = -\infty$. (c) Schematic diagram of the *temporal* evolution of the potential vorticity interface [$L(x, 0) = 0$] when a small amplitude constriction (the stipled "strait") is suddenly moved leftward at $t = 0$ with a uniform subcritical speed. The transverse velocities v forced at $t = 0$ tend to deflect the interface to $L(x, t_1)$, and this generates relative vorticities whose sense is indicated by the circular arrows. These vortices cause the interface to propagate to $L(x, t_2)$ for $t_2 > t_1$. As $t \rightarrow \infty$ the ridge ahead of the constriction continues propagating to $x = -\infty$, whereas the trough remains behind in equilibrium with the v forced by the constriction, as shown in (a).

and the solution that vanishes at $D = 1$ is

$$2L = \left(D - \frac{1}{\zeta} \right)$$

$$- \left[\left(D - \frac{1}{\zeta} \right)^2 - 4(1 - D)/\zeta \right]^{1/2} > 0. \quad (2.7)$$

The minimum width D_c of the strait necessary for blocking in this case is given by setting the discriminant equal to zero, that is,

$$0 = \left(D_c - \frac{1}{\zeta} \right)^2 - 4(1 - D_c)/\zeta \equiv \left(D_c + \frac{1}{\zeta} \right)^2 - \frac{4}{\zeta}, \quad (2.8)$$

and therefore

$$D_c = 2\zeta^{-1/2} - \zeta^{-1} = 2 \left(\frac{R}{\beta - 1} \right)^{1/2} - \frac{R}{\beta - 1}. \quad (2.9)$$

For large W_1 Eqs. (2.2)–(2.4a) also imply

$$U_1 \rightarrow 1, \quad (2.9a)$$

which is obviously required to satisfy the transport relation $W_1 U_1 = W_1$ in the wide ($W_1 \gg 1$) region.

The question arises as to the physical consistency of an *inviscid* escarpment model, and its relation to a model with slightly smoother topography. Accordingly, the critical value for (2.4b) has been compared (in the Appendix) with the corresponding value for a model having a smoother continental slope. The numerical results indicate that the inviscid escarpment limit is approached asymptotically for large finite continental slopes (in which case the lateral viscous stresses might be consistently neglected.) This justification of the escarpment model is necessary because it provides the only tractable nonlinear theory for obtaining the new upstream state when the old one is blocked, as will be seen. Before proceeding to this question, a physical explanation of Fig. 3a, and motivating arguments for Fig. 4 are in order.

The appearance of a steady-state "trough" (i.e., $L > 0$ in Fig. 3a) can be qualitatively explained in terms of well-known (e.g., Stern 1991) properties of free and forced topographic *long* waves. Consider the evolution from time $t = 0$ when the fluid is resting with $L(x, 0) = 0$, and then the strait (constriction) is moved leftward with uniform speed (Fig. 3c). This obviously forces an *initial* transverse velocity $v > 0$ at $x < 0$, and $v < 0$ at $x > 0$, so that the potential vorticity interface at small $t_1 > 0$ is deflected as shown. The vorticity generated by the cross-escarpment displacement then causes relative leftward phase (and group) propagation of L if the relative upstream velocity is subcritical (i.e., smaller than the propagation speed of free topographic long waves). Therefore, at $t_2 > t_1$ the L-ridge moves ahead of the strait and continues propagating to $x = -\infty$ as an unforced (free) wave. But the advance of the trough eventually ceases under the influence of the forced v, and thus the steady-state trough $L > 0$ (Fig. 3a) is attained in the strait.

This picture applies to small values of $(1 - D_m)$, and for larger ones a first-order nonlinear hyperbolic equation (Stern 1991) applies to the evolutionary problem. In this case the current in the converging strait may increase to a value such that the "local L-propa-

gation speed" (according to the method of characteristics) vanishes, at which point (x) the trailing edge of the ridge remains behind in the vicinity of the strait, while the leading edge continues propagating to $x = -\infty$ in the locally subcritical region ($D \approx 1$). Figure 4 is a schematic diagram of this conjectured flow, as seen by an observer on the strait. As $t \to \infty$ the upstream propagating blocking ridge ($\lambda > 0$) produces a new mean field with an anticyclonic shear layer at all finite $x < 0$. Farther downstream a transition to the supercritical branch (cf. Fig. 3b) of the new steady solution occurs, with cyclonic vorticity appearing in the trough region (Fig. 4). This (incomplete) picture of the temporal evolution provides the motivation for the following "self-consistent" *steady* long-wave theory.

Let x_0 in Fig. 4 denote the (unknown) zero crossing point of the interface, let D_0 denote its distance from the curved wall, and let U_0'' denote the (unknown) horizontal velocity at x_0. This velocity must have the same value in both layers because $L(D_0) = 0$ implies that there is no vorticity at x_0. Since the total volume transport between the two walls must have the same value at all t, x (even at $x = \pm\infty$ in the transient region), it follows that the transport $U_0'' D_0 \beta + U_0'' W_1$ at x_0 must equal the original transport $W_1 + \beta$ at $x = -\infty$, or

$$U_0'' = \frac{1 + \beta/W_1}{1 + \beta D_0/W_1}. \tag{2.10}$$

Let $L(x) \geq 0$ be the interface displacement in the $x \geq x_0$ region, and let $\lambda(x) \geq 0$ be the interface displacement in the $x < x_0$ region. By applying mass conservation to the former region (as done previously), and using $L(D_0) = 0$, a solution for $L(D)$ is obtained containing one unknown (U_0''). Since the blocking condition $\min D < D_c$ is satisfied, the solution requires a branch point with $\partial L/\partial D = \infty$, and with $\partial L/\partial x = (\partial L/\partial D)(\partial D/\partial x)$ finite. Therefore the branch point must
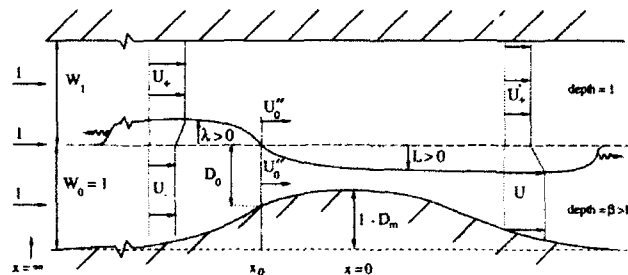

FIG. 4. The modification of the upstream flow by a topographic blocking wave. The minimum width D_m of the deep channel is at $x = 0$. A wiggly arrow indicates the upstream propagation of the anticyclonic vorticity ($\zeta_- > 0$) layer of thickness $\lambda(x) > 0$. This produces a reduction of the lower-layer velocity (U_-) relative to the undisturbed velocity ($=1$) at $x = -\infty$. At $x > x_0$ a compensating cyclonic vorticity ($\zeta > 0$) of thickness $L(x) > 0$ develops downstream. At large *finite* distances upstream from the obstacle, and at large finite time after startup, a steady state is assumed, even though the blocking wave continues propagating to $x \to -\infty$.

occur where $\partial D/\partial x = 0$, that is, at $x = 0$ where $D = D_m$ (Fig. 4), or

$$\left(\frac{\partial D}{\partial L}\right)_{D_m} = 0. \tag{2.11}$$

This equation determines the final unknown in the $L = L(D)$ solution, and gives the new downstream velocity field. With D_0 and U_0'' known, the mass balance for $x < x_0$ gives $\lambda(D)$ and the new vorticity field upstream from the strait.

This outline of the calculation will now be carried out for the simplest case of large W_1 [cf. Eq. (2.7)], in which case the upper-layer velocity (2.9a) is nearly equal to unity ($U_0 = 1$) at all x, and $U = 1 + \zeta L$ beneath the interface in the cyclonic ($x > x_0$) region. The steady mass balance for this region then becomes $(1 + \zeta L)(D - L) = D_0$, or

$$L^2 - L\left(D - \frac{1}{\zeta}\right) + (D_0 - D)/\zeta = 0. \tag{2.12}$$

For the (β, R) values listed subsequently, the zero-crossing point is at $x_0 < 0$ and therefore $D < D_0$ in $x_0 < x < 0$. Since $L > 0$ as $D - D_0 \to 0^-$, Eq. (2.12) requires

$$D_0 > \frac{1}{\zeta} = \frac{R}{\beta - 1}, \tag{2.13}$$

and therefore, the solution that vanishes at x_0 is

$$2L = \left(D - \frac{1}{\zeta}\right) - \left[\left(D - \frac{1}{\zeta}\right)^2 - 4(D_0 - D)/\zeta\right]^{1/2} > 0. \tag{2.14}$$

Downstream from the branch point ($x = 0$) defined by (2.11) the appropriate solution of (2.12) is

$$2L = \left(D - \frac{1}{\zeta}\right) + \left[\left(D - \frac{1}{\zeta}\right)^2 - 4(D_0 - D)/\zeta\right]^{1/2} \tag{2.15}$$

and the branch point ($D = D_m$) occurs where the discriminant vanishes, or

$$0 = \left(D_m - \frac{1}{\zeta}\right)^2 - 4(D_0 - D_m)/\zeta$$

$$= \left(D_m + \frac{1}{\zeta}\right)^2 - \frac{4D_0}{\zeta}.$$

Therefore the zero-crossing point of the interface occurs where

$$D_0 = \frac{\zeta}{4}\left(D_m + \frac{1}{\zeta}\right)^2. \tag{2.16}$$

Equations (2.14)–(2.16) give the new downstream state ($L > 0$) after blocking occurs; but (2.13) restricts

the solution to the parametric regime $1 < \zeta D_0 = (\zeta D_m / 2 + 1/2)^2$, or $\zeta D_m > 1$, and by combining this with (2.9) we get

$$\zeta^{-1} < D_m < 2\zeta^{-1/2} - \zeta^{-1} \qquad (2.17)$$

$$\zeta = \frac{\beta - 1}{R} > 1$$

for the restricted D_m range.

The $\lambda \geq 0$ solution for $x \leq x_0$ is obtained by noting that $U_- = 1 - \lambda \zeta_-$ is the velocity below the escarpment in Fig. 4, where $\zeta_- = \zeta/\beta$. Therefore the total transport below the interface is

$$D\beta U_- + \frac{1}{2}(1 + U_-)\lambda = D_0\beta$$

or

$$\lambda^2 - 2\lambda\left(\frac{1}{\zeta_-} - \beta D\right) - \frac{2\beta}{\zeta_-}(D - D_0) = 0, \quad (2.18)$$

$$1 > D > D_0 > D_m > \frac{1}{\zeta}. \qquad (2.19)$$

These inequalities imply $\zeta_-^{-1} - \beta D < 0$, and therefore the solution of (2.18) satisfying $\lambda \geq 0$ is

$$\lambda = \frac{1}{\zeta_-} - \beta D + \left[\left(\frac{1}{\zeta_-} - \beta D\right)^2 + 2\beta(D - D_0)/\zeta_-\right]^{1/2}. \qquad (2.20)$$

At $x < x_0$, $U_- = 1 - \lambda\zeta_-$ becomes

$$U_- = D\zeta - (\zeta^2 D^2 - 2\zeta D_0 + 1)^{1/2}, \quad (2.21)$$

and far upstream ($D \to 1$) the velocity is

$$U_-(-\infty) = \zeta - (\zeta^2 - 2\zeta D_0 + 1)^{1/2}, \quad (2.22)$$

where D_0 is given by (2.16).

These results may be summarized as follows. No blocking occurs when the minimum channel width D_m exceeds the upper bound in (2.17), and in this case the original upstream flow merely produces a symmetrical trough $L(x) \geq 0$ in the vicinity of the obstacle. When D_m is *slightly* less than the upper bound in (2.17), Eq. (2.16) gives $D_0 \to 1$, which means $x_0 \to -\infty$, $\lambda \approx 0^+$, and $L(x) > 0$ at all x. But there is a branch point at $x = 0$, and a transition from (2.14) to (2.15), so that at $x = +\infty$ we get $2L = 2(1 - 1/\zeta) > 0$. If D_m is decreased further below the upper bound in (2.17) then $D_0 < 1$ in (2.16), x_0 becomes finite negative, $\lambda(x) > 0$, and a finite modification of the upstream state (Fig. 4) occurs in which anticyclonic vorticity appears, in addition to the cyclonic vorticity in the $L > 0$ strip which extends far downstream. When D_m equals the lower bound (ζ^{-1}) in (2.17) then $D_0 = 1/\zeta = D_m$ so that $x_0 = 0$, and the modified upstream velocity (2.22) is

$$U_- = \zeta - (\zeta^2 - 1)^{1/2} < 1.$$

If D_m is less than the lower bound in (2.17) then a sign change in x_0 is suggested (by the above value of $x_0 = 0$), in which case a separate calculation is necessary. The foregoing calculation also does not apply when R exceeds the bound in (2.5b), because the current at $x = -\infty$ is strong enough to prevent upstream topographic wave propagation.

This steady longwave theory neglects the possibility of persistent *short* wave effects, such as are bound to occur (as "shocks") in the temporal evolution. These eddy effects might be studied in a finite difference computation using a smooth continental slope model, such as appears in the Appendix.

3. The two-escarpment model of a strait

Figure 2 has a greater geometric resemblance to a strait, and a jetlike ($L_1 > 0$, $L_2 > 0$) solution is sought when $W_1 = 1 = W_2$ provide the length scale. The cyclonic vorticity ζ is given by (1.1), and the (magnitude of the) anticyclonic vorticity ζ_- is given by (1.2). The uniform velocities on the upper and lower shelf are given, respectively, by $U_1 = U - \zeta L_1$, $U_2 = U - L_2\zeta_-$, where U is the uniform velocity between the interfaces. What is min(D) for a hydraulic or for a separating transition in this model?

For the lowest layer (Fig. 2) of uniform potential vorticity and unit depth the total volume transport ($U - L_2\zeta_-)(1 - L_2)$ at any $D(x)$ must equal unity, or

$$U = \frac{1}{1 - L_2} + L_2\zeta_-. \qquad (3.1)$$

In the middle layer between the two interfaces, the total volume transport $\beta U(D - L_1) + (U - L_2\zeta_-/2)L_2$ equals βW_0, or

$$L_1 U = UD - W_0 + \beta^{-1}(U - L_2\zeta_-/2)L_2. \qquad (3.2)$$

In the uppermost layer the transport balance is

$$U - \zeta L_1 + \beta(U - \zeta L_1/2)L_1 = 1. \qquad (3.3)$$

The values of (β, R, W_0) necessary to justify the $L_1 > 0$, $L_2 > 0$ assumption are obtained by letting $x \to -\infty$, $L_1 \to 0$, $L_2 \to 0$, $U - 1 \equiv \mu \to 0$, $W_0 - D \equiv 2M(x) \to 0^+$. In this region the linearization of (3.1)–(3.3) yields

$$\mu = (1 + \zeta_-)L_2,$$

$$L_1 = \mu W_0 - 2M + \beta^{-1}L_2,$$

$$\mu = (\zeta - \beta)L_1,$$

and consequently

$$L_2 = -\frac{2M(\zeta - \beta)}{1 + \zeta_- - (\zeta - \beta)[(1 + \zeta_-)W_0 + \beta^{-1}]}, \qquad (3.4)$$

$$L_1 = \frac{1 + \zeta_-}{\zeta - \beta}L_2.$$

The last equation requires

$$\beta < \zeta = \frac{\beta - 1}{R}, \qquad (3.5)$$

and since $M > 0$ Eq. (3.4) requires

$$(\zeta - \beta)[(1 + \zeta_-)W_0 + \beta^{-1}] - (1 + \zeta_-) > 0. \qquad (3.6)$$

When this is multiplied by β and when $\beta\zeta_- = \zeta$ is used, we get

$$(\zeta - \beta)[(\zeta + \beta)W_0 + 1] - (\zeta + \beta) > 0$$

or

$$\beta^2 + \frac{2\beta}{W_0} < \zeta^2 = \frac{(\beta - 1)^2}{R^2}. \qquad (3.7)$$

This condition for positive (L_1, L_2), as well as the one in (3.5) is obviously satisfied for sufficiently small Rossby number.

The significance of (3.7) appears by considering the conditions under which the basic flow at $x = -\infty$ can support a free (i.e., $M(x) \equiv 0$) *stationary* long wave of infinitesimal amplitude. Equation (3.4) implies that this will occur when the denominator vanishes, or when the left-hand side of (3.6) vanishes, or when an equality sign replaces the inequality in (3.7). The latter equality then gives the Rossby number for a stationary long wave, and for smaller R the long wave propagates upstream. It is under the latter condition (3.7) that a steady forced solution with $L_1 > 0$, $L_2 > 0$ for $D(x) < W_0$ is obtained. (See the previous argument in connection with Fig. 3c.)

TABLE 1a. Critical values of the parameters for the two escarpment model (section 3 and Fig. 2) when $\beta = 2$, and for various values of R, W_0. The first row for each entry is the minimum D, and the following rows are U_1, U, U_2, respectively. The symbol H indicates a hydraulic or blocking transition.

| R | W₀ | | | | |
	1	2	4	8	32
1/4	.85 H	1.40 H	2.5 H	4.68 H	26.08 H
	.544	.168	.178	.170	.769
	1.455	1.831	1.821	1.829	1.230
	1.167	1.332	1.327	1.331	1.080
1/6	.68 H	1.16 H	2.12 H	4.36 H	15.68 H
	.383	.302	.294	.426	.303
	1.961	2.068	2.078	1.903	2.066
	1.288	1.327	1.331	1.268	1.326
1/10	.52 H	.92 H	1.72 H	3.30 H	12.8 H
	.386	.389	.389	.380	.377
	2.507	2.501	2.500	2.517	2.524
	1.313	1.312	1.311	1.316	1.317
1/20	.36 H	.62 H	1.24 H	2.2 H	8.64 H
	.340	.286	.417	.283	.304
	3.647	3.787	3.439	3.795	3.742
	1.305	1.326	1.276	1.327	1.319

TABLE 1b. Same as Table 1a except $\beta = 1.5$. The symbol S indicates a separation transition. A blank entry indicates no transition (the upstream flow is not subcritical).

| R | W₀ | | | | |
	1	2	4	8	32
1/4	—	1.88 H	3.14 S	5.6 S	22.7 H
		.355	.036	.016	.245
		1.358	1.603	1.619	1.439
		1.167	1.297	1.306	1.209
1/6	.91 H	1.51 H	2.60 H	4.80 H	27.8 H
	.703	.2435	.176	.179	.847
	1.296	1.756	1.823	1.820	1.152
	1.105	1.297	1.328	1.327	1.052
1/10	.70 H	1.16 H	2.12 H	4.00 H	15.0 H
	.51	.31	.35	.344	.314
	1.875	2.165	2.107	2.119	2.16
	1.236	1.332	1.312	1.316	1.33
1/20	.48 H	.82 H	1.48 H	2.88 H	10.8 H
	.344	.358	.338	.371	.342
	2.975	2.945	2.998	2.918	2.980
	1.328	1.322	1.333	1.316	1.329

It will now be shown that neither L_1 nor L_2 can change sign farther downstream in the region where their amplitudes are finite. Suppose the contrary were true, and let x' denote the smallest x at which either L_1 or L_2 vanish. If $L_2(x') = 0$ with $L_1(x') > 0$ then (3.1) yields $U = 1$, and (3.2) yields $D = W_0 + L_1 > W_0$, which contradicts the initial assumption (Fig. 2) that $D(x) \le W_0$. If, on the other hand, $L_1(x') = 0$ with $L_2(x') > 0$ then (3.3) gives $U = 1$, whereas (3.1) gives $U > 1$, and thus a contradiction is again obtained. Therefore all admissable solutions of the nonlinear equations (3.1)–(3.3) have positive L_1, L_2 if (3.7) is satisfied.

The solution of the nonlinear equations is obtained by multiplying (3.1) with $1 - L_2$, by multiplying (3.3) with $(1 - L_2)^3 U^2$, and by eliminating both $L_1 U$ and U from (3.3) to obtain a seventh-order polynomial equation for the single unknown L_2. The very large number of terms in the coefficients of this polynomial were assembled by a symbolic computer program, and then the L_2 root was computed by a careful numerical search for the zero-crossing point of the polynomial. Since this starts from a point far upstream where L_2 is very small, very small L_2 increments must be taken in the search, and then small D increments must be taken to remain on the same branch of the seventh-order polynomial as one proceeds downstream. The run terminates at that $D = D_{crit}$ for which there is either no root ("hydraulic transition" point) or one of the velocities (U_1) turns negative ("separation"). Tables 1a,b,c list the solution for various values of β, R, W_0, and the letter H or S indicates the type of critical point. For example, when $\beta = 1.5$ (Table 1b), $R = 1/10$, $W_0 = 1$, a hydraulic transition (H) occurs (first) when the

TABLE 1c. Same as Tables 1a, 1b except $\beta = 1.25$.

R	W_0 1	2	4	8	32
1/4	—	—	—	—	—
1/6	—	—	—	6.08 S .027 1.527 1.271	21.6 S .007 1.543 1.280
1/10	.94 H .758 1.241 1.084	1.59 H .336 1.663 1.256	2.68 H .174 1.825 1.329	4.88 H .179 1.820 1.327	18.24 H .198 1.801 1.318
1/20	.67 H .546 1.981 1.230	1.12 H .410 2.209 1.295	1.96 H .336 2.327 1.331	3.68 H .337 2.326 1.331	14.0 H .347 2.311 1.326

minimum channel width is $D = 0.70$, and at this section $U_1 = 0.51$, $U = 1.875$, $U_2 = 1.236$. The accuracy of the roots was checked by using those values to compute the local volume flux, and by comparing the result with the flux at $x = -\infty$.

The downstream evolution of the jet is illustrated in Fig. 5a for $W_0 = 8$, $R = \frac{1}{6}$, $\beta = 1.5$. This shows that as x increases from $-\infty$ (where $D = 8$), the value of U_1 decreases and a hydraulic transition point occurs at $D = 4.80$ with $\min U_1 > 0$. At a larger R (Fig. 5b), with other things being equal, a separation ($U_1 = 0$) transition occurs first at $D = 5.6$. In both cases a jet ($U > U_2 > U_1$) forms, but Tables 1a,b,c indicate that the separation regime is relatively restricted, occurring only for the larger Rossby numbers and for the smaller topographic effect ($\beta - 1$). The table also shows that decreasing R, with fixed W_0 and β, requires a decreasing D_{crit} (i.e., a greater strait convergence) for a critical state, and the accompanying maximum jet velocity U is increased.

When blocking occurs in Fig. 2 the new state that arises could be obtained by generalizing the procedure in section 2, but the algebra then becomes formidable.

Interesting variations in Fig. 2 and Fig. 4 might be obtained by less restrictive shelf widths (W_1, W_2), in which case separation might be more prevalent. The effect of a sill might be obtained by allowing β to vary with D. It may also be possible to replace the rigid bottom in the central channel (Fig. 2) by an interface beneath which the fluid density increases, and above which the potential vorticity is (piecewise) uniform. Then the important role of buoyancy on the blocking could be ascertained.

4. Conclusions

A jet can be generated by inviscid cross-isobath flow through the converging half of a strait, and two types of transition may allow the generated vorticity to ap-

pear in the diverging half. The local flow may become hydraulically critical in which case the generated topographic blocking wave modifies the upstream state as well as the downstream state (Fig. 4 and section 2). In the second kind of transition an everywhere subcritical jet may separate because of the relative vorticity generated in the narrow part of the strait [cf. Fig. 5b and Stern and Whitehead (1990)].

Both transitions are examples of purely inertial (as contrasted with diffusive) mechanisms for generating inshore vorticity in the passage of currents through straits. They may therefore be relevant to the explanation of the large *cyclonic* vorticity in the Straits of Florida, and to the explanation of the reformation of the western boundary jet in the vicinity of the Straits of Yucatan.
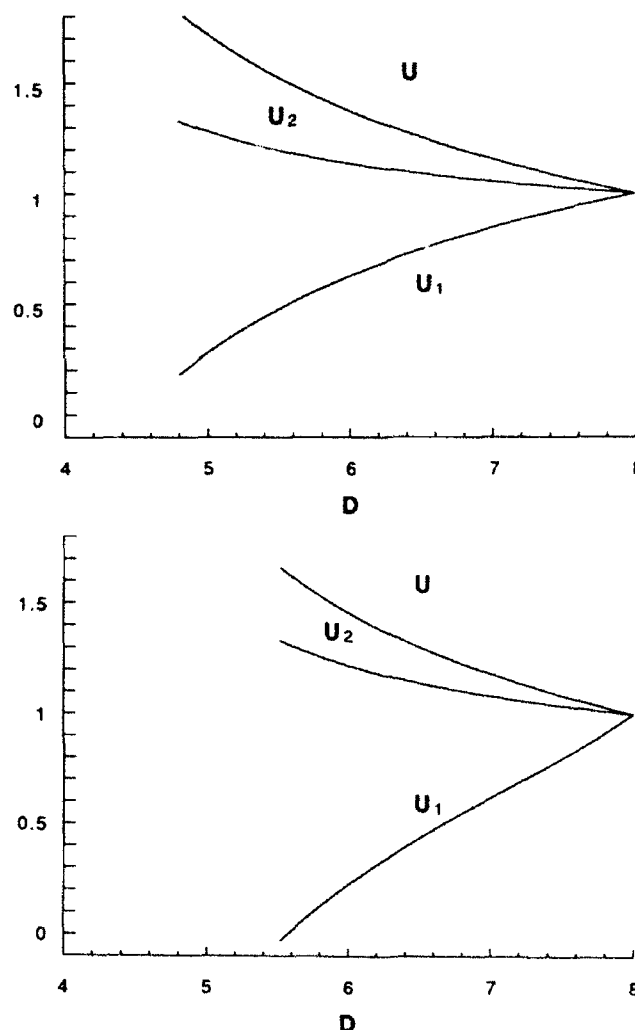

FIG. 5. (a) Downstream variation of velocity in Fig. 2 when $\min D(x)$ equals the critical value for a hydraulic transition, and when $W_0 = 8 = D(-\infty)$, $R = \frac{1}{6}$, $\beta = 1.5$. U_1 is the uniform velocity on the upper shelf, U_2 is the velocity on the lower shelf, and U is the uniform velocity between the two potential vorticity interfaces. A jet with $U > U_2$, $U > U_1$ forms at the transition point $D = 4.8$. (b) Same as (a) except that $R = \frac{1}{4}$. In this case a separation transition ($U_1 = 0$) at $D = 5.6$ occurs before a hydraulic transition.

Similar kinds of transitions could occur in a purely continental type of topography (cf. Stern 1991, Fig. 2), such as is obtained by removing the sidewall in deep water and curving the sidewall on the shelf. I would like to take this opportunity to correct an omission in that paper (Stern 1991). A term $\check{r}$ sinh$k\epsilon$ + cosh$k\epsilon$ should appear in the denominator of the integral of Eq. (4.9), but this term equals unity in the long-wave ($k \to 0$) limit, and consequently the omission affects none of the equations following (4.9).

APPENDIX

A Smooth Continental Slope

For previously mentioned reasons it is important to compare the critical blocking condition for the escarpment model in Fig. 3a with the value obtained for a smoother nondimensional cross-stream topography $h(y)$ that is also independent of x. For this calculation it is convenient to take the distance $W_1 = 1$ of the upper wall from the $y = 0$ datum (defined below) as the unit of length, with $y = -D(x)$ as the ordinate of the curved lower wall, and with $D(-\infty) = W_0$ as a free parameter. The uniform velocity at $x = -\infty$ is again taken as the velocity unit, that is, $U_0 = 1$.

If $\theta = \theta(y)$ denotes the ordinate at $x = -\infty$ of the steady streamline whose ordinate is y at $D(x)$, then the Lagrangian volume conservation equation in nondimensional units is

$$u(y) = q \frac{d\theta}{dy}, \qquad (A.1)$$

$$q = \frac{h(\theta)}{h(y)}, \qquad (A.2)$$

and the potential vorticity conservation equation is

$$-\frac{du}{dy} = \frac{1}{R}\left(\frac{1}{q} - 1\right), \qquad (A.3)$$

where

$$R = \frac{U_0}{f W_1^*}. \qquad (A.4)$$

The solution of (A.1)–(A.3) for $y = y(\theta)$ must satisfy the boundary conditions

$$y(1) = 1, \qquad (A.5)$$

$$y(-W_0) = -D(x), \qquad (A.6)$$

for a given W_0 and for each $D = D(x)$. The numerical solution is greatly facilitated by replacing (A.6) with an assigned value of $u(1)$, and then "marching" to θ = $-W_0$, at which point the computed y gives the value of D for each $u(1)$. The calculation proceeds with successively smaller values of $u(1) < 1$ until the minimum

TABLE 2. Minimum channel width ($D - D_{crit}$) for blocking as a function of the inverse continental slope (s). Here $u(-D)$ is the corresponding velocity at the curved (lower) wall, and $u(1)$ is the velocity at the upper wall; $R = 1/30$, $\beta = 1.5$, $W_0 = 1$. See Appendix for definitions.

s	D_{crit}	$u(1)$	$u(-D)$
∞	.50	.42	3.3
10	.499	.400	3.29
5	.513	.222	3.30
2.5	.535	.286	2.71
1	.687	.166	1.43

D [as a function of $u(1)$] is reached. This gives the critical amplitude of the obstacle necessary to block the upstream flow, and to cause a hydraulic transition.

Calculations were made for the hyperbolic tangent profile

$$h(y) = -p \tanh(sy) + p \tanh s + 1, \qquad (A.7)$$

$$p \equiv \frac{\beta - 1}{\tanh(sW_0) + \tanh s},$$

whose maximum slope defines the $y = 0$ datum level, and which satisfies $h(1) = 1$, $h(-W_0) = \beta$. The free parameter s is a measure of the inverse width of the continental slope, and $s \to \infty$ gives the escarpment limit in Fig. 3a.

A second-order Runge–Kutta integration was used to solve Eqs. (A.1)–(A.3), and the step size used was checked by comparing the total volume transport at x with an analytic calculation at $x = -\infty$. Table 2 gives the results for four finite s when $W_0 = 1$, $R = 1/30$, $\beta = 1.5$. The $s = \infty$ entry was obtained from (2.4b) for the escarpment model in section 2, and we conclude that the critical value of D for blocking is essentially the same in the interval $5 < s < \infty$, thereby validating the asymptotic consistency of the escarpment model.

REFERENCES

Brooks, I. H., and P. P. Niiler, 1977: Energetics of the Florida Current. *J. Mar. Res.*, **35**, 163–191.

Gill, A. E., 1977: The hydraulics of rotating channel flow. *J. Fluid Mech.*, **80**, 651–671.

Gordon, A. L., 1967: Circulation of the Caribbean Sea. *J. Geophys. Res.*, **72**(24), 6207–6223.

Hughes, R. L., 1985: Multiple criticalities in coastal flow. *Dyn. Atmos. Oceans*, **9**, 321–340.

——, 1986: On the role of criticality in coastal flows over irregular bottom topography. *Dyn. Atmos. Oceans*, **10**, 129–147.

——, 1987: The role of the higher shelf modes in coastal hydraulics. *J. Mar. Res.*, **45**, 33–58.

Long, R., 1972: Finite amplitude disturbances in flow/over obstacles. *Ann. Rev. Fluid Mech.*, **4**, 69–92.

Molinari, R. L., M. Spillane, I. Brooks, A. Atwood, and C. Duckett, 1981: Surface currents in the Caribbean Sea. *J. Geophys. Res.*, **86**, 6537–6542.

Stern, M. E., 1991: Countergradient vorticity flux in continental boundary currents. *J. Phys. Oceanogr.*, **21**, 1622–1630.

Stern, M. E., and J. Whitehead, 1990: Separation of a boundary jet in a rotating fluid. *J. Fluid Mech.*, **217**, 41–69.